CSIRO PUBLISHING
www.publish.csiro.au/journals/pasa *Publications of the Astronomical Society of Australia*, 2006, **23**, 69–75

An Atomic and Molecular Study of the Interstellar Medium Around the Supernova Remnant RCW 103

Sergio A. Paron[A,D], *Estela M. Reynoso*[A], *Cormac Purcell*[B], *Gloria M. Dubner*[A], *and Anne Green*[C]

[A] Instituto de Astronomía y Física del Espacio (IAFE), 1428 Buenos Aires, Argentina
[B] Department of Astrophysics and Optics, University of New South Wales, Sydney NSW 2052, Australia
[C] School of Physics, University of Sydney, Sydney NSW 2006, Australia
[D] Correspondence author. E-mail: sparon@iafe.uba.ar

Received 2006 January 10, accepted 2006 March 22

Abstract: We report on the detection of HCO^+ and ^{12}CO emission in the rotational transition $J = 1–0$ in the vicinity of the shock front at the southern border of the supernova remnant RCW 103, where previous infrared observations suggest an interaction with a molecular cloud. The observations were carried out with the Australian Millimeter Radiotelescope at Mopra. We observed a depletion of HCO^+ behind the supernova shock front. In addition, we studied the interstellar medium over an extended region towards RCW 103 based on archival λ 21 cm HI line observations from the Australia Telescope Compact Array (ATCA) and the Parkes Telescope. No atomic gas was observed in emission in coincidence with the molecular feature. This absence was interpreted in terms of self-absorption processes.

Keywords: ISM: molecules — ISM: clouds — ISM: supernova remnants — supernova remnants: individual (G332.4-0.4, RCW 103)

1 Introduction

Supernova remnants (SNRs) mark the catastrophic death of massive stars, and they modify irreversibly the surrounding medium into which the shock front is expanding. Roughly half of all Galactic SNRs are located near large molecular clouds (Huang & Thaddeus 1986), presumably the parent clouds of the massive stellar progenitors. When an SNR interacts with a molecular cloud, the shock wave depletes and excites molecular species, significantly altering the local chemistry.

RCW 103 (G332.4-0.4) is a Galactic SNR that shows clear evidence of an interaction with a molecular cloud near its southern limb. At radio wavelengths, this SNR appears as an almost complete circular shell with a diameter of 8′ (Caswell et al. 1980). Optical filaments are seen towards the brightest regions of the radio shell (van den Bergh et al. 1973; Ruiz 1983). Based on HI absorption measurements, Caswell et al. (1975) estimated a distance of 3.3 kpc for RCW 103. Using this distance, Carter et al. (1997) studied the expansion of the optical filaments and calculated an age for the remnant of about 2000 years. In X-rays, RCW 103 presents a structure compatible with shell SNRs in the young double-shock stage of their evolution (Chevalier 1982).

Figure 1a shows a radio continuum image of RCW 103 at 1.4 GHz from Reynoso et al. (2004), and Figure 1b a soft X-ray image extracted from the *Chandra* Supernova Remnant Catalog. Good concordance is observed between the non-thermal radio emission and the soft X-ray emission. A compact central object (CCO) has been detected in hard X-rays (Gotthelf et al. 1999) near R.A. $16^h17^m35^s$, dec. –51° 02′ 25″ (J2000) with no detected radio counterpart. There are strong indications that this CCO is part of a binary system (e.g., Becker & Aschenbach 2002).

Observations in the 2.122 μm line of the H_2 and other near infrared lines (Burton & Spyromilio 1993; Oliva et al. 1990), suggest that the remnant is interacting with molecular material on the southern side. Burton and Spyromilio conclude that the H_2 spectrum of RCW 103 is typical of dense gas ($\geq 10^5$ cm^{-3}) collisionally excited by low velocity (10–20 km s^{-1}) shocks. In a recent paper, Chevalier (2005) suggests that RCW 103 is not embedded in a molecular cloud, but rather that the blast wave is interacting with previous circumstellar material swept up by the progenitor star.

In a search for shocked molecular gas near the southern border of RCW 103 we carried out observations in two molecular lines: ^{12}CO $J = 1–0$ and HCO^+ $J = 1–0$. The former is the brightest molecular line, very sensitive to the presence of molecular gas. Its detection confirms the existence of molecular concentrations on the southern side of RCW 103. HCO^+ emission is enhanced at high densities and this molecule is particularly sensitive to shock emission, providing a good tracer of the shock location. However, this line is generally quite weak.

The interstellar HCO^+ ion has been extensively studied in the past. In well-shielded regions, where interstellar radiation plays a minor role (molecular regions), the dominant reactions that produce HCO^+ are the following: H_2 + Cosmic Rays → $H^+ + H + e^-$, then $H^+ + H_2 \rightarrow H_3^+$,

 10.1071/AS06003 1323-3580/05/02144

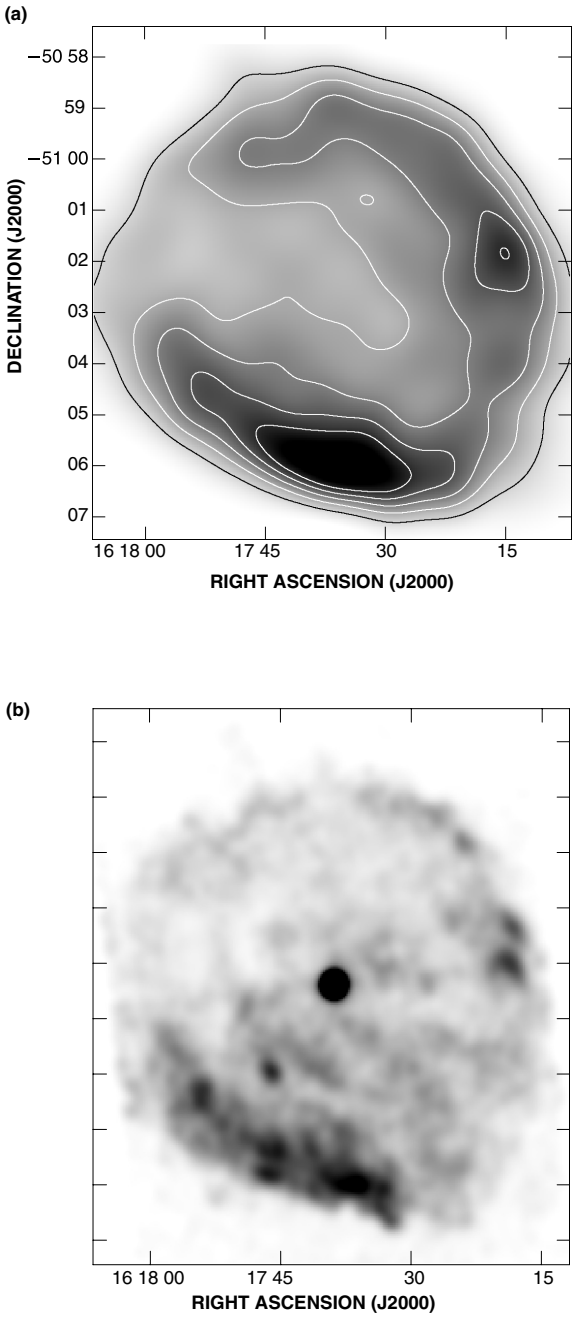

Figure 1 (a) Non-thermal radio emission from RCW 103 at 1.4 GHz (Reynoso et al. 2004). The contour levels are 0.1, 0.2, 0.3, 0.4, and 0.5 Jy beam^{-1}. (b) Soft X-ray emission in the energy band 1.6–3.0 keV (*Chandra* Supernova Remnant Catalog).

and finally $H_3^+ + CO \rightarrow HCO^+ + H_2$. There is much controversy in the literature about the way in which shocks modify the HCO^+ chemistry. Iglesias & Silk (1978) showed that HCO^+ must be depleted behind slow shocks. However, HCO^+ observations towards IC443 showed an abundance enhancement of this molecule behind the supernova shock front (e.g., Dickinson et al. 1980). Elitzur (1983) proposed that this enhancement resulted from increased ionization due to cosmic rays trapped by shock-compressed magnetic fields. However, subsequent observations of IC443 (Ziurys et al. 1989; van Dishoeck et al. 1993) showed that the HCO^+ abundance in the shocked gas is not significantly enhanced compared with pre-shocked values.

In this paper we investigate the interplay between RCW 103 and its surrounding medium based on observations of ^{12}CO and HCO^+. A complementary analysis of HI λ 21 cm data is also presented.

2 Observations

2.1 Millimetre Line Observations

We observed the $J = 1–0$ rotational transitions of ^{12}CO ($\nu = 115$ GHz) and HCO^+ ($\nu = 89$ GHz) using the 22-m Mopra antenna, near Coonabarabran, Australia. Spectra were recorded in position-switching mode, with the telescope alternating between the target and an emission-free reference position. The back-end consisted of an auto-correlator, configured to have a bandwidth of 64 MHz divided into 1024 channels, which provided a velocity resolution of $\sim$0.2 kms^{-1} over a usable bandwidth of $\sim$120 kms^{-1}. The pointing accuracy was checked before each mapping run by observing a nearby SiO maser, and is estimated to be better than 10″. Nine pointings, at constant right ascension (R.A. = $16^h17^m37^s$) were observed towards the southern rim of RCW 103 with a resolution of $\sim$34″. Pointings were spaced at 30″ intervals in declination, from –51° 05′ 30″ to –51° 09′ 30″ (Figure 2a). Also in Figure 2b, we include a radio continuum and an X-ray emission profile at constant Right Ascension (R.A. = $16^h17^m37^s$) to show the SNR shock front position. In this picture, the SNR outer shell peaks at dec. –51° 6′, and the intensity decreases towards the shell centre (smaller negative declinations) on the left side of the plot. The crosses with numbers at the top indicate the positions of the molecular line observations, and correspond to the numbered profiles in Figure 3. Pointings 1 and 2 lie inside the SNR, pointing 3 is at the rim (as seen in radio wavelengths), and the rest probe gas external to the remnant.

2.2 HI Observations

The λ 21 cm HI data used in the present paper are described in detail in Reynoso et al. (2004). These observations were carried out using the Australia Telescope Compact Array (ATCA) in the 750A array of a 1° × 1° region around RCW 103, during a 12 h run on 2002 January 22. The baselines in this array range from 76.5 to 735 m. A second observation of 12 h with the telescope in the EW 367 array (baselines from 46 to 367 m) took place on 2002 April 1. The angular resolution of the combined data is 50″. A correlator configuration of 1024 channels was used with a total bandwidth of 4 MHz centered at 1420 MHz. The velocity resolution at this frequency is 1 km s^{-1}. Continuum data were obtained simultaneously with a bandwidth of 128 MHz centered at 1384 MHz. Single dish data from the Southern Galactic Plane Survey (SGPS; McClure-Griffiths et al. 2005) in the 21 cm HI line were added in order to recover the contribution from lower spatial frequencies.

https://doi.org/10.1071/AS06003 Published online by Cambridge University Press

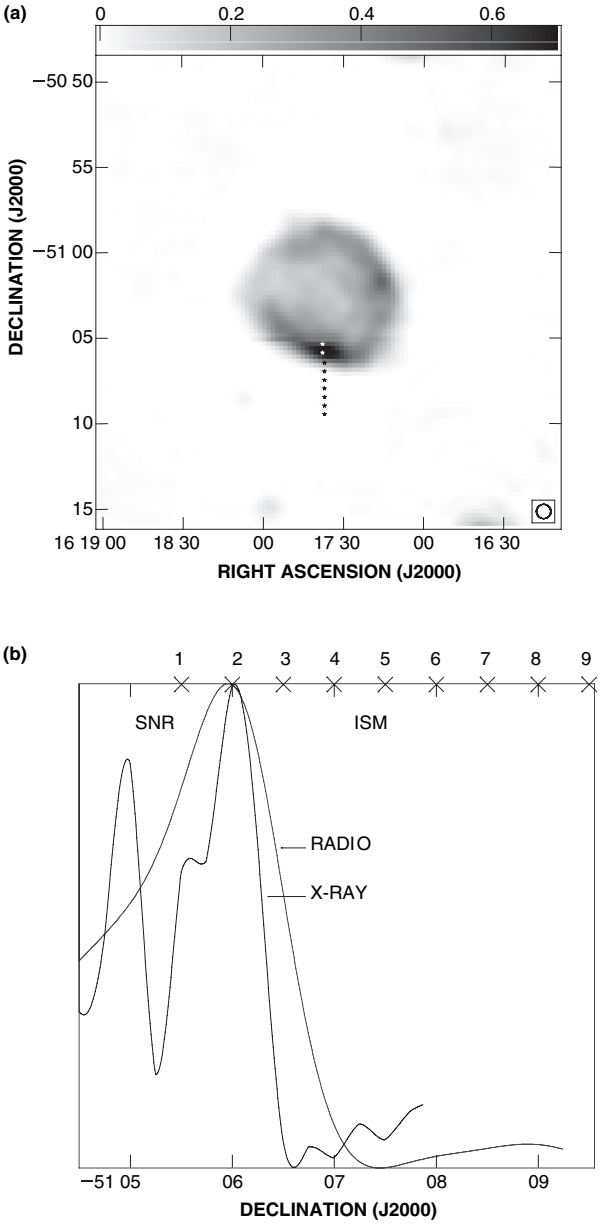

Figure 2 (a) Radio continuum emission at 1.4 GHz in an extended field around RCW 103 (Reynoso et al. 2004). The nine dots towards the South of the SNR indicate the pointings for the molecular line observations. The grayscale is in units of Jy beam^{-1}. The beam, $50'' \times 50''$, is plotted in the bottom right corner. The rms noise level of this image is 5.5 mJy beam^{-1}. (b) A line profile at constant R.A. ($16^h17^m37^s$) for 1.4 GHz radio continuum and X rays (1.6–3.0 keV, from *Chandra* Supernova Remnant Catalog). The crosses with numbers on top indicate the pointings of the molecular line observations.

3 Results

3.1 Molecular Gas

Figure 3 displays all the observed profiles in the $J = 1$–0 transition of ^{12}CO and HCO$^+$ in the velocity range between –60 km s^{-1} and –20 km s^{-1}. In this velocity interval, the ^{12}CO spectra have several components, with the brightest one centered near –48 km s^{-1}. The HCO$^+$ spectra are, as expected, simpler with only one conspicuous feature centered at a velocity varying between –45 and –50 km s^{-1} along the pointings, broadly in coincidence with the most intense ^{12}CO peak (all kinematical velocities in this paper are referred to the LSR).

In Table 1 we present the observed parameters of the molecular line components peaking near 48 km s^{-1}. The peak temperatures (T_{peak}), central velocities (V_c) and velocity widths (Δv) were obtained from Gaussian fits to the main components of the spectra. The ^{12}CO central velocities correspond to the most intense peaks. The rms noise is $\sigma_{CO} \sim 0.15$ K and $\sigma_{HCO^+} \sim 0.02$ K. The last column represents the ratio between the HCO$^+$ and ^{12}CO peak temperatures.

3.2 Atomic Gas

Figure 4 shows the distribution of HI in grayscale from $v = -75$ to +43 km s^{-1} integrated in 10 km s^{-1} steps. The contours correspond to the radio continuum emission of RCW 103. These velocity slices reveal the patchy appearance of the cold gas in the surroundings of RCW 103. The hole in the emission evident in the map at –21.3 km s^{-1}, corresponds to absorption by the Sagittarius-Carina Galactic arm, whose distance is ~1.5 kpc. Since HCO$^+$ is observed only between –52 and –43 km s^{-1}, Figure 5 shows the HI λ 21 cm emission integrated over this velocity range to determine if there is an atomic gas counterpart to the molecular feature. There is a hint of a shell of atomic gas open to the NE of the SNR, and a structure partially overlaping the remnant towards the East. Assuming that the gas is optically thin and using the relation $N(\mathrm{HI}) = 1.82 \times 10^{18} \int T_B \, dv$, where T_B is the brightness temperature, the HI column density integrated in the above velocity range is estimated to be $N(\mathrm{HI}) \sim 1.6 \times 10^{21}$ cm^{-2} for the shell and the East clump. Based on these values and assuming a distance of 3.3 kpc for RCW 103 (from section 4.2), we calculate an HI mass ~800 $M_\odot$ for the East clump and aproximately 4400 $M_\odot$ for the open shell. Curiously, no atomic gas is detected close to the southern border of RCW 103 down to a detection level of 3σ. This finding is discussed later.

4 Discussion

4.1 Molecular Gas

From Figure 3, it is clear that the HCO$^+$ intensity decreases from outside to the interior of the SNR shell, with the emission being weakest for the pointings 1 to 3. The coincidence between the shock front position and the change in the HCO$^+$ intensity strongly suggests the existence of a physical interaction between the SNR and the molecular gas. To investigate if such a change is the consequence of the passage of the shock front or is simply due to a decrease in the ambient molecular density, it is necessary to compare the HCO$^+$ emission with that of another molecule that remains unnaffected by the shock passage. For that purpose, we compared the HCO$^+$ emssion with that of ^{12}CO. The use of ^{12}CO as a reference molecule may be problematic because the

https://doi.org/10.1071/AS06003 Published online by Cambridge University Press

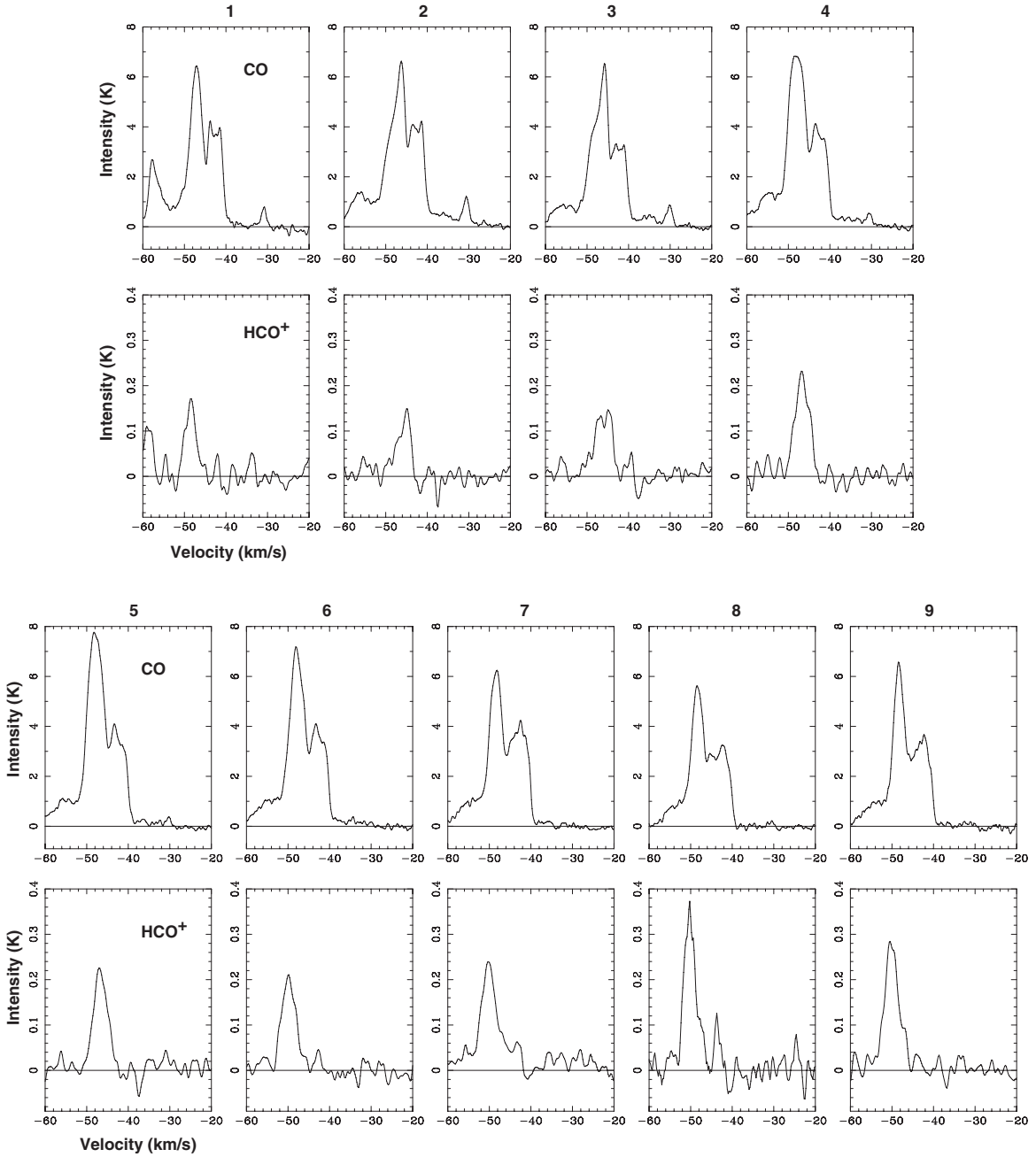

Figure 3 The ^{12}CO and HCO$^+$ spectra are displayed in pairs with the ^{12}CO profiles in the upper panel and HCO$^+$ in the lower one for every pointing, numbered as in Figure 2. The plotted velocity range is [–60 km s^{-1}, –20 km s^{-1}] for both molecular transitions. The temperature scales vary from –1 to 8 K for ^{12}CO and from –0.1 to 0.4 K for HCO$^+$.

excitation conditions between ^{12}CO and a high dipole moment species like HCO$^+$ could be different. However, assuming that ^{12}CO and HCO$^+$ are uniformly mixed, the comparison would be meaningful. We find that the $T^{\rm HCO^+}/T^{\rm ^{12}CO}$ ratio is lower for pointings 1 to 3 than for those that lie well beyond the SNR shock front. For the inner pointings, the lower values in the intensity of the HCO$^+$ emission are probably indicative of shock depletion of this molecule. Thus, our results confirm that the SNR shock affects the chemistry of the molecular gas, but do not support models that predict HCO$^+$ enhancement by the passage of a shock.

However, the decrement is not as low as that predicted by the Iglesias & Silk (1978) model, which produces a decrease of two orders of magnitude in the HCO$^+$ abundance behind a shock front, on time scales of 1000 yr and for shock velocities of $\sim$10 km s^{-1}. A short interaction time or a shock front with different velocity could explain the smaller decrease observed in the HCO$^+$ emission behind the shock, as compared to the theoretical predictions. Nevertheless, to determine the HCO$^+$ abundance accurately, it would be useful to observe a higher dipole moment molecule, such as HCN, rather than ^{12}CO (see Ziurys et al. 1989) for the reference molecule.

https://doi.org/10.1071/AS06003 Published online by Cambridge University Press

Table 1. Observed and derived parameters

Pointing	T_{peak} [K]		V_c[km s^{-1}]		Δv [km s^{-1}]		$T^{HCO^+}/T^{^{12}CO}(\times 10^{-2})$
	^{12}CO	HCO$^+$	^{12}CO	HCO$^+$	^{12}CO	HCO$^+$	
1	6.60	0.15	−47.1	−49.0	3.6	1.8	2.2
2	6.60	0.15	−46.1	−45.3	3.6	3.7	2.2
3	6.50	0.15	−46.4	−46.7	4.3	5.6	2.3
4	6.90	0.23	−48.2	−47.2	4.3	3.7	3.3
5	7.80	0.23	−48.2	−46.7	4.3	4.7	2.9
6	7.20	0.23	−48.2	−49.5	4.3	4.7	3.1
7	6.30	0.23	−48.2	−49.9	5.1	4.7	3.6
8	5.60	0.40	−48.2	−50.0	4.3	3.7	7.1
9	6.70	0.30	−48.6	−49.5	4.3	3.7	4.4

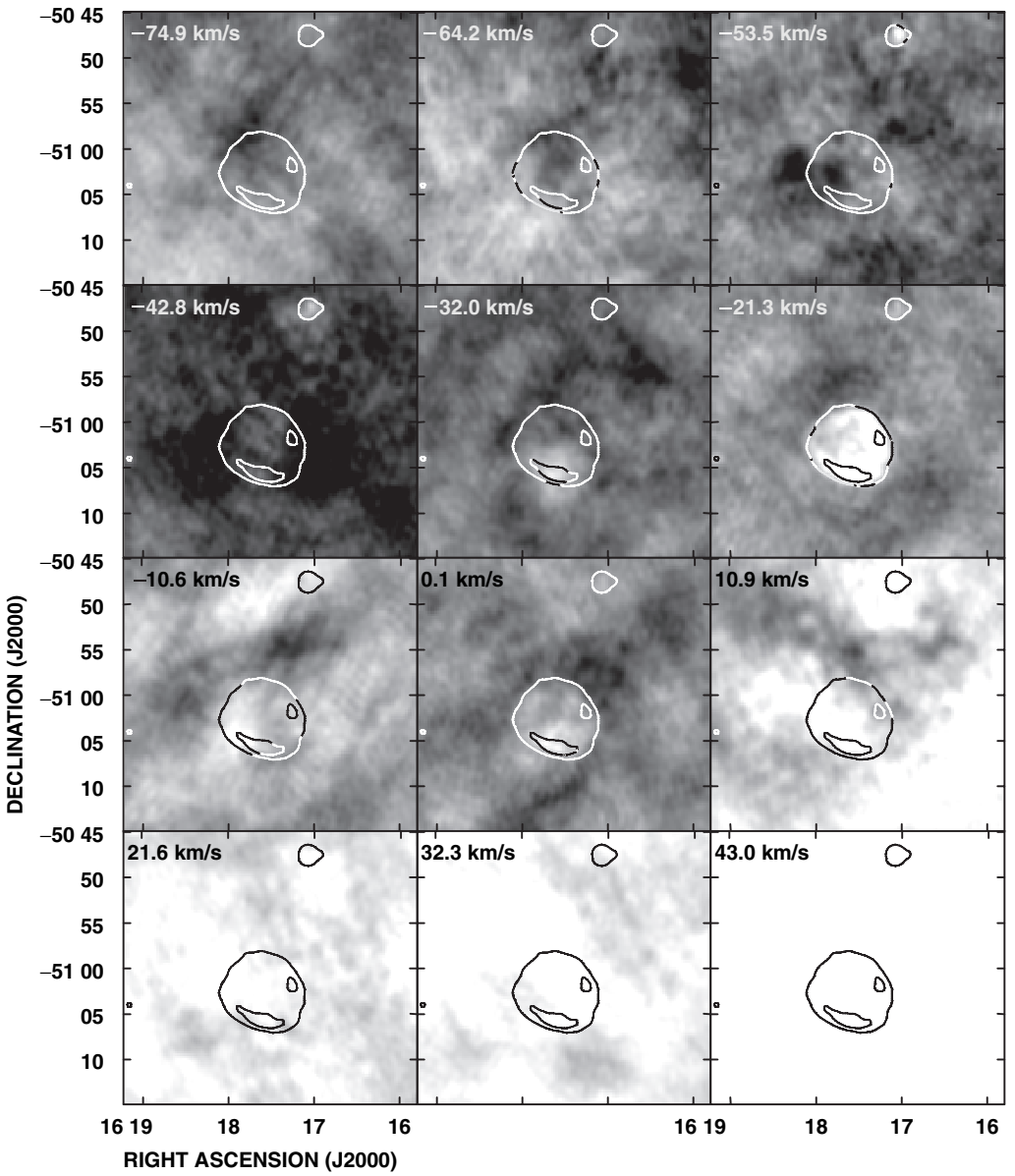

Figure 4 HI images between –75 and +43 km s^{-1}, each one integrated over ∼10 km s^{-1}. The velocity shown in the upper left corner of each image corresponds to the first channel of integration. The grayscale ranges from 400 to 1200 K km s^{-1}. A few contours of the radio continuum of RCW 103 are included for comparison.

https://doi.org/10.1071/AS06003 Published online by Cambridge University Press

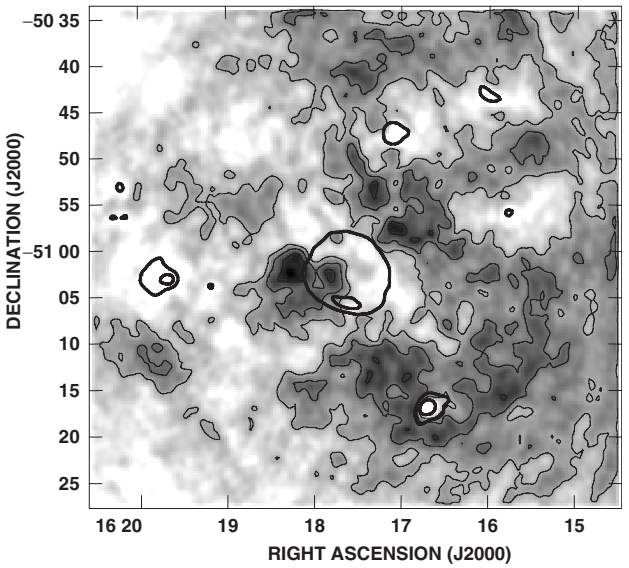

Figure 5. Total HI λ 21 cm emission integrated between –52 and –43 km s^{-1}. The grayscale varies between 650 and 1100 K km s^{-1}. Contours at 800, 900, 1000, and 1050 K km s^{-1} are included to emphasize the morphology of the atomic gas. A few contours from the radio continuum image of RCW 103 are shown for comparison. The rms noise level of the image is ∼47 K km s^{-1} and the resolution is $50'' \times 50''$.

4.2 Kinematical Distance

Previous distance studies suggested a range of possible values between 3.1 and 4.6 kpc for RCW 103 (Reynoso et al. 2004). The velocity at which the HCO^+ emission is produced, coincident with that of the most intense ^{12}CO peak, allows us to constrain the systemic velocity of RCW 103 to about –48 km s^{-1}. This velocity corresponds to a distance of ∼3.3 kpc using the Galactic rotation model of Fich et al. (1989).

4.3 Atomic Gas

From Figure 4 and Figure 5, it is clear that on the southern side of RCW 103, where the remnant may be interacting with a molecular cloud, we do not observe dense HI emission adjacent to the SN shock. It is possible that the lack of HI emission in this region is not due to the absence of atomic hydrogen, but to self-absorption processes, as can be seen in Tycho's SNR. Proper motion measurements (Reynoso et al. 1997) showed that the lowest shock expansion velocities around the outer shell of Tycho's SNR are found to the East, and it was suggested that a higher ambient density was decelerating the expansion in this direction. However, a subsequent study (Reynoso et al. 1999) detected faint HI emission in this region. The observations can be explained if a cooler HI component is self-absorbing a warmer one. Lee et al. (2004) confirmed this hypothesis with detection of the molecular emission counterpart of the HI self-absorption. The presence of ambient, unshocked molecular gas is indicative of low temperatures. A similar scenario for

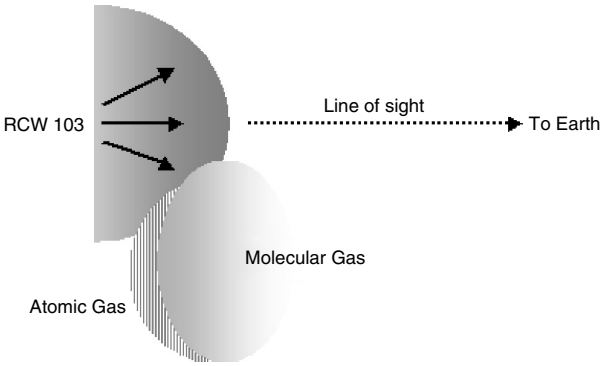

Figure 6 A schematic model of the RCW 103 interaction with a molecular cloud to the South.

RCW 103 also is consistent with Burton & Spyromilio's (1993) model, in which a reverse shock is propagating back into the swept-up atomic gas following the interaction of the blast wave with a dense molecular cloud. The blast wave is propagating at 15 km s^{-1} and the molecular cloud is located ahead of the neutral hydrogen mass. Moreover, since the reverse shock has already overrun the HI cloud, the shocked gas will be much warmer than the unshocked gas which is mixed with the molecular ambient cloud, thus producing the observed self-absorption. In this context, the eastern HI clump could be part of an extended structure which has a uniform temperature and for which the emission is not self-absorbed. A sketch of the possible gas distribution is shown in Figure 6. The cool molecular component appears closer to us than the warmer atomic gas and the supernova shock front is currently running into the molecular cloud.

In Reynoso et al. (2004), the absorption spectrum towards RCW 103 was analyzed by applying different filtering techniques. In their figure 2, an absorption feature that was seen well above the noise (>6σ) at +34 km s^{-1}, disappeared after deeper filtering and hence, was considered not to be caused by absorption against the continuum emission from RCW 103. To review a possible association with RCW 103, a map of the HI distribution at this velocity was produced.

Figure 7 shows the HI distribution integrated within 4 km s^{-1} around +34 km s^{-1}. The neutral gas depicts an open shell-like structure well-matched to the SNR ring. Since the molecular data presented here and the HI absorption study in Reynoso et al. (2004) have shown that the systemic velocity of RCW 103 is –48 km s^{-1}, it is highly unlikely that this HI shell at +34 km s^{-1} (which corresponds to a kinematic distance of 19 kpc using the Galactic rotation model of Fich et al. 1989) has been driven by the SN shock front.

Although there is a good morphological match between the radio continuum extent and the HI feature, it is very difficult to explain any relationship between the SNR and this HI structure. The most likely explanation is chance juxtaposition and no relationship.

https://doi.org/10.1071/AS06003 Published online by Cambridge University Press

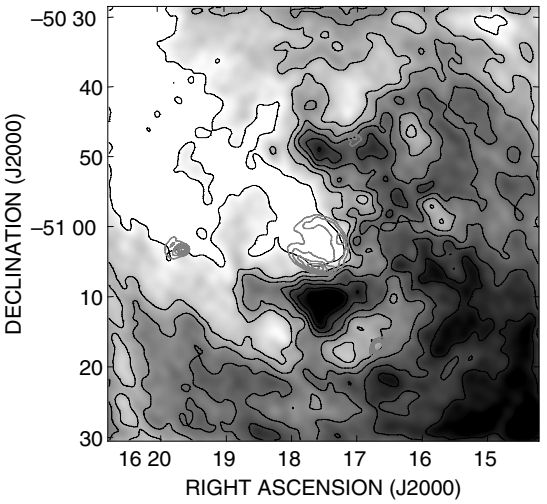

Figure 7 HI emission integrated within 4 km s^{-1} around +34 km s^{-1}. The grayscale varies between 30 and 70 K km s^{-1}. The HI contour levels (in black) are 30, 40, 50, 60 and 65 K km s^{-1}. A few contours (in grey) representing the radio continuum of RCW 103 are shown for comparison.

5 Summary

We have investigated the interstellar medium around the SNR RCW 103. The present ^{12}CO $J = 1$–0 and HCO^+ $J = 1$–0 observations provide new evidence for an interaction between the SNR and a molecular cloud. We also investigated the surrounding atomic gas based on the λ 21 cm HI line. The main results can be summarized as follows:

(a) From $J = 1$–0 ^{12}CO and HCO^+ observations towards the southern side of RCW 103, we find that the HCO^+ spectra have only a single component which has the same kinematical velocity of $\sim$ –48 km s^{-1} as the brightest feature observed in the ^{12}CO spectrum.

(b) The $T^{HCO^+}/T^{^{12}CO}$ ratio at this velocity range has lower values for the interior pointings (1 to 3) than for those that are well away from the SNR shock front. The low ratio values for the innner positions may be due to HCO^+ depletion caused by the remnant shock front colliding with the molecular gas.

(c) The molecular observations allows us to constrain the systemic velocity of RCW 103 to about –48 km s^{-1}. This velocity corresponds to a distance of $\sim$3.3 kpc for the remnant, using the Galactic rotation model of Fich et al. (1989).

(d) We do not detect HI emission on the southern side of the remnant at –48 km s^{-1}, where molecular gas is observed. We suggest that this result is due to self-absorption processes, similar to those observed in Tycho's SNR.

Acknowledgments

We thank Michael Burton for help with the molecular line proposal. S.A.P. thanks Facundo Albacete for a fruitful discussion about the X-ray image. S.A.P. is a fellow of CONICET, Argentina. E.M.R. and G.D. are members of the Carrera del Investigador Científico, CONICET, Argentina. During part of this work, E.M.R. was a visiting scholar at the University of Sydney. This research was partially funded through the Australian Research Council, by the UBACYT Grant A055 and by ANPCyT-PICT04-14018 (Argentina). The ATCA is funded by the Commonwealth of Australia for operation as a National Facility by CSIRO.

References

Becker, W. & Aschenbach, B. 2002, in Proceedings of the 270 WE-Heraeus Seminar on Neutron Stars, Pulsars, and Supernova Remnants, 278, MPE Report, eds. W. Becker, H. Lesch, and J. Trümper (Garching: Max-Plank-Institut für extraterrestrische Physik), 64
Burton, M., & Spyromilio, J. 1993, PASA, 10, 327
Carter, L. M., Dickel, J. R., & Bomans, D. J. 1997, PASP, 109, 990
Caswell, J. L., Haynes, R. F., Milne, D. K., & Wellington, K. J. 1980, MNRAS, 190, 881
Caswell, J. L., Murray, J. D., Roger, R. S., Cole, D. J., & Cooke, D. J. 1975, A&A, 45, 239
Chevalier, R. A. 1982, ApJ, 258, 790
Chevalier, R. A. 2005, ApJ, 619, 839
Dickinson, D. F., Dinger, A. S. C., Kuiper, T. B. H., & Rodriguez Kuiper, E. N. 1980, ApJ, 237, L43
Elitzur, M. 1983, ApJ, 267, 174
Fich, M., Blitz, L., & Stark, A. A. 1989, ApJ, 342, 272
Gotthelf, E. V., Petre, R., & Vasisht, G. 1999, ApJ, 514, L107
Huang, Y.-L., & Thaddeus, P. 1986, ApJ, 309, 804
Iglesias, E. R. & Silk, J. 1978, ApJ, 226, 851
Lee, J., Koo, B., & Tatematsu, K. 2004, ApJ, 605, L113
McClure-Griffiths, N. M., Dickey, J. M., Gaensler, B. M., Green, A. J., Haverkorn, M., & Strasser, S. 2005, ApJS, 158, 178
Oliva, E., Moorwood, A. F. M., & Danziger, I. J. 1990, A&A, 240, 453
Reynoso, E. M., Green, A. J., Johnston, S., Goss, W. M., Dubner, G. M., & Giacani, E. B. 2004, PASA, 21, 82
Reynoso, E. M., Moffett, D. A., Goss, W. M., Dubner, G. M., Dickel, J. R., Reynolds, S. P., & Giacani, E. B. 1997, ApJ, 491, 816
Reynoso, E. M., Veláquez, P. F., Dubner, G. M., & Goss, W. M. 1999, AJ, 117, 1827
Ruiz, M. T. 1983, AJ, 88, 1210
van den Bergh, S., Marscher, A. P., & Terzian, Y. 1973, ApJS, 26, 19
van Dishoeck, E. F., Jansen, D. J., & Phillips, T. G. 1993, A&A, 279, 541
Ziurys, L. M., Snell, R. L., & Dickman, R. L. 1989, ApJ, 341, 857

https://doi.org/10.1071/AS06003 Published online by Cambridge University Press